Energy Conversion and Management 103 (2015) 739–751

Contents lists available at ScienceDirect

Energy Conversion and Management

journal homepage: www.elsevier.com/locate/enconman

Operation optimization of a distributed energy system considering energy costs and exergy efficiency

M. Di Somma [a,c,*], B. Yan [b], N. Bianco [a], G. Graditi [c], P.B. Luh [b], L. Mongibello [c], V. Naso [a]

[a] Dipartimento di Ingegneria Industriale (DII), Università degli studi Federico II, P.le Tecchio, Napoli 80125, Italy
[b] Department of Electrical and Computer Engineering, University of Connecticut, Storrs, CT 06269, USA
[c] ENEA – Italian National Agency for New Technologies, Energy and Sustainable Economic Development, CR Portici, 80055 Portici, Italy

ARTICLE INFO

Article history:
Received 17 February 2015
Accepted 4 July 2015
Available online xxxx

Keywords:
Operation optimization
Distributed energy systems
Energy costs
Exergy efficiency

ABSTRACT

With the growing demand of energy on a worldwide scale, improving the efficiency of energy resource use has become one of the key challenges. Application of exergy principles in the context of building energy supply systems can achieve rational use of energy resources by taking into account the different quality levels of energy resources as well as those of building demands. This paper is on the operation optimization of a Distributed Energy System (DES). The model involves multiple energy devices that convert a set of primary energy carriers with different energy quality levels to meet given time-varying user demands at different energy quality levels. By promoting the usage of low-temperature energy sources to satisfy low-quality thermal energy demands, the waste of high-quality energy resources can be reduced, thereby improving the overall exergy efficiency. To consider the economic factor as well, a multi-objective linear programming problem is formulated. The Pareto frontier, including the best possible trade-offs between the economic and exergetic objectives, is obtained by minimizing a weighted sum of the total energy cost and total primary exergy input using branch-and-cut. The operation strategies of the DES under different weights for the two objectives are discussed. The operators of DESs can choose the operation strategy from the Pareto frontier based on costs, essential in the short run, and sustainability, crucial in the long run. The contribution of each energy device in reducing energy costs and the total exergy input is also analyzed. In addition, results show that the energy cost can be much reduced and the overall exergy efficiency can be significantly improved by the optimized operation of the DES as compared with the conventional energy supply system using the grid power only.

1. Introduction

With the growing demand of energy on a worldwide scale, improving the efficiency of energy resource use has become one of the key challenges. The consumption of primary energy in buildings accounts for more than one third of the total world's energy consumption [1]. Most of the energy used in buildings is required to maintain room temperatures at around 20–26 °C, or to heat water at a temperature around 60 °C. These thermal demands are commonly supplied by electricity or fossil sources [1,2]. Assessments of energy use in buildings are usually based on quantitative considerations by using the First Law of Thermodynamics [1]. Concerning the conservation of energy, the First Law, however, does not take into account the degradation of the energy quality that takes place when high-quality energy resources, such as electricity or fossil fuels, are used to satisfy low quality thermal demands.

Exergy, derived from the Second Law of Thermodynamics, is a measure of the energy quality. It is the maximum amount of work that can be obtained from an energy flow as it comes to the equilibrium with the reference environment [1,3–7], and can be viewed as the potential of a given energy amount. Unlike energy, exergy is not subject to conservation (except for reversible processes). Rather, exergy is destroyed due to irreversibilities in any real process [8]. Exergy analysis was used for performance evaluation of single energy systems, e.g., geothermal systems [9–11], cogeneration systems [12–15], renewable energy sources [16], and heat recovery steam generators [17], with the aim to find the most rational use of energy. The performances of different options of

* Corresponding author at: Dipartimento di Ingegneria Industriale (DII), Università degli studi Federico II, P.le Tecchio, Napoli 80125, Italy. Tel.: +39 081 7723204; fax: +39 3492963733.

E-mail addresses: marialaura.disomma@enea.it, marialaura.disomma@unina.it (M. Di Somma).

http://dx.doi.org/10.1016/j.enconman.2015.07.009
0196-8904/

Nomenclature

A	area (m^2)
$\dot{B}$	biomass mass flow rate (kg/h)
c	constant in Eq. (29) (kW h/$)
$\dot{C}$	cooling rate (kW)
COP	coefficient of performance
$Cost$	total energy cost ($)
DR	maximum ramp-down rate (kW)
ex_{bio}	specific chemical exergy of biomass (kW h/kg)
ex_{gas}	specifical chemical exergy of natural gas (kW h/Nm^3)
$\dot{E}$	electricity rate (kW)
Ex	exergy (kJ)
$\dot{Ex}$	exergy rate (kW)
F_{obj}	objective function
F_q	Carnot factor
$\dot{G}$	natural gas volumetric flow rate (Nm^3/h)
$\dot{G}_T$	total solar irradiance (kW/m^2)
$\dot{H}$	heating rate (kW)
H	thermal energy (kW h)
k	generation level of the energy device (kW)
LHV_{bio}	lower heat value of biomass (kW h/kg)
LHV_{gas}	lower heat value of gas (kW h/Nm^3)
P_{bio}	biomass price ($/t)
P_{gas}	natural gas price ($/$Nm^3$)
P_{grid}	electricity price ($/kW h)
$\dot{Q}_{GT,ex}$	heat rate made available by the exhaust gas (kW)
t	time (h)
T	temperature (K)
UR	maximum ramp-up rate (kW)
x	binary decision variable

Greek symbols

Δt	length of the time interval (h)
ε_{gen}	exergy efficiency of electricity generation
ς	exergy factor
η	efficiency
μ	percent heat loss rate of the gas turbine
ξ	gas turbine exhaust fraction
ϕ_{sto}	storage loss fraction
ψ	overall exergy efficiency
ω	weight in Eq. (29)

Superscript/subscripts

0	reference
abs	absorption chiller
bio	biomass
boil	boiler
buy	bought
CCHP	combined cooling, heating and power
coll	collector
dem	demand
DHW	domestic hot water
di	directly provided by natural gas
e	electricity
ED	energy device
EH	electrical heater
ex	exhaust gas
gas	natural gas
GT	gas turbine
HP	heat pump
HR	heat recovery
in	input
max	maximum
min	minimum
out	output
req	required
SC	space cooling
SH	space heating
solar	solar
source	energy resource
sto	thermal storage
th	thermal

Acronyms

CCHP	combined cooling, heating and power
DES	distributed energy system

energy supply systems to meet building demands were evaluated and compared in terms of exergy efficiencies in [18–20]. The concept of exergy was introduced to the building environment by Björk et al. [21], Kilkiş [22] and Molinari [23,24]. In buildings, energy demands are characterized by different energy quality levels. Since the required temperatures for space heating and cooling are low, the quality of these energy demands is low. The energy quality needed for the production of domestic hot water at about 60 °C is slightly higher than that for space heating or cooling. For electrical appliances and lighting, the highest possible quality of energy is needed. Exergy analysis may promote the matching of quality levels of supply and demand, by covering if possible low quality thermal demands with low exergy sources, e.g., solar thermal or waste heat of power generation processes, and electricity demands with high exergy sources. In this way, the waste of high-quality energy resources can be significantly reduced. Therefore, exergy modeling explicitly exposes the irreversibility aspect of energy use, and exergy optimization then allows increasing world's sustainability, crucial in the long run, through efficient use of energy while considering energy qualities.

A Distributed Energy System (DES) refers to an energy system where energy is made available close to energy consumers, typically relying on a number of small-scale technologies [25]. In recent years, developing DES has attracted much interest. One of the benefits of DESs is the possibility to integrate different energy resources, including renewable ones [26–30], as well as to recover low-temperature waste heat for thermal use [31]. In these applications, DESs, as the smallest units to match the quality levels of supply and demand, provide a unique opportunity to obtain the benefits of exergy analysis. However, most of the studies in the literature are focused on the operation optimization of DESs to reduce energy costs, which is essential in the short run. Among them, integrated optimization of energy devices and energy processes of a small eco-community was carried out in Yan et al. [32] to reduce the total daily energy cost. The solution methodology used was branch-and-cut. A mixed-integer optimization model for scheduling multiple energy devices connected to a low energy building was developed in Guan et al. [33] to minimize the overall costs of electricity and natural gas. The problem was also solved by branch-and-cut. Beyond minimizing costs only, optimized operation strategies to reduce energy costs and CO_2 emissions were analyzed. In [34], a mixed-integer model for a small building cluster was established, and the surrogate Lagrangian relaxation method was used to solve the multi-objective problem. In [35], a multi-objective linear problem was programmed in the LINGO software, and the compromise programming method was employed to solve it.

Exergy was considered in multi-carrier energy systems in Ramirex-Elizondo et al. [36] and Krause et al. [37], with the aim to maximize the overall exergy efficiency defined as the ratio of the total exergy required to meet the given energy demands to the total primary exergy input to the system. In both papers, the demands were not time-varying. In [36], the problems were solved by using the "fmincon constraint nonlinear optimization solver" available in the Matlab optimization toolbox. Results obtained by minimizing energy costs and maximizing the overall exergy efficiency were compared. As expected, the best solution in terms of the overall exergy efficiency was different from the most economical solution. No direct relation between the exergetic and the economic optimization was found.

The operation optimization of a DES to satisfy given time-varying user demands, in order to obtain a rational use of energy resources considering exergy and energy costs, is presented in this paper. The energy devices in the DES under consideration are chosen from commonly used ones: biomass boiler, solar thermal plant, Combined Cooling Heating and Power (CCHP), reversible heat pump, and thermal energy storage. A set of primary energy carriers with different energy quality levels are converted to meet given time-varying user demands with different energy quality levels. A multi-objective linear programming problem is formulated. The economic objective is formulated as the total energy cost to be minimized, given the time-of-day electricity prices and constant natural gas and biomass prices. The exergetic objective is to maximize the overall exergy efficiency of the DES. Since energy demands are assumed known, the total exergy required to meet the demands is also known, and the overall exergy efficiency can be increased by reducing the exergy input to the DES. Therefore, the exergetic objective is formulated as the total primary exergy input to be minimized. Preliminary results presented in [38] are extended in the present paper. The Pareto frontiers, consisting of the best possible trade-offs between the energy costs, essential in the short run, and the overall exergy efficiency crucial in the long run, are obtained for a representative winter and summer day, and the operators of the DES can choose the operation strategy from the Pareto frontiers based on short- and long-run priorities. The performance of the DES in terms of energy costs and overall exergy efficiency are compared with those of a conventional energy supply system, where all the energy demands are met by the grid power. The problem is solved by using branch-and-cut. The model is implemented by using IBM ILOG CPLEX Optimization Studio Version 12.5.

Results of numerical testing show that the minimization of primary exergy input promotes an efficient energy supply system where all the energy resources, including renewable ones, are used in an efficient way. The optimized operation allows reducing energy costs and primary exergy input as compared with conventional energy supply systems. Moreover, the contribution of each energy device in reduction of energy costs and primary exergy input are discussed, and the operation strategies of the DES under different weights for the two objectives are presented.

In the following, Section 2 is on the modeling of the DES and the economic objective. The exergetic objective and the multi-objective optimization method are described in Section 3. Results are presented and discussed in Section 4.

2. Problem formulation

The DES under consideration consists of conversion energy devices, thermal storage systems, and different types of end-user demands, interconnected via different energy carriers. The energy devices are chosen among the most commonly used ones in practical DESs. Fig. 1 shows the scheme of the DES with possible routes of energy flows from various energy resources with different energy quality levels via energy conversion and storage systems to meet demands with different exergy requirements. Primary energy devices (gas turbine, biomass boiler, solar thermal plant) convert a set of primary input energy carriers into electricity and heat. Secondary energy devices (reversible heat pump, heat recovery boilers, absorption chiller) convert electricity and heat for heating and cooling. To allow more efficient use of thermal energy, a thermal storage section is included in the DES. A multi-objective linear programming problem is formulated below. Modeling of energy devices and thermal storages, modeling of energy balance, and the economic objective are presented in Subsections 2.1, 2.2, and 2.3, respectively. The exergetic objective is presented later in Section 3.

2.1. Modeling of energy devices and thermal storages

In this subsection, the modeling of the biomass boiler, solar thermal plant, CCHP system, reversible heat pump and thermal energy storage is presented. It is assumed that the energy devices involved in the DES have constant efficiencies, although the efficiencies actually depend on partial loads. The constant-efficiency assumption for energy devices is systematically used in the scientific literature for design and operation optimization problems of large-scale DESs to maintain the problem linearity [31,35,39–42]. For biomass boiler, heat recovery boilers, heat pump, and gas turbine generator, the common constraint is the capacity constraint. For simple presentation, this general constraint is described as follows. If the energy device, *ED*, is in use, (the on/off binary decision variable $x_{ED}(t)$ is equal to 1), its generation level, $k_{ED}(t)$ (a continuous decision variable), has to be within the minimum value, $k_{ED}^{\min}$, and the capacity, $k_{ED}^{\max}$, i.e.,

$$x_{ED}(t)\cdot k_{ED}^{\min} \leqslant k_{ED}(t) \leqslant x_{ED}(t)\cdot k_{ED}^{\max}, \text{ for all } t. \tag{1}$$

Additional constraints of each device are considered below.

2.1.1. Modeling of the biomass boiler

A biomass boiler is used to meet the demand of domestic hot water. The mass flow rate in the biomass boiler, $\dot{B}_{boil}(t)$, is given by:

$$\dot{B}_{boil}(t) = \dot{H}_{bio}(t)/(\eta_{boil,bio}\cdot LHV_{bio}), \text{ for all } t, \tag{2}$$

where $\dot{H}_{bio}(t)$ is the heat generation level of the biomass boiler, $\eta_{boil,bio}$ the combustion efficiency of the boiler, and LHV_{bio} the lower heat value of the biomass.

2.1.2. Modeling of the solar thermal plant

The solar thermal plant is also used to meet the demand of domestic hot water. The heat generation level of the solar plant, $\dot{H}_{solar}(t)$, is [41]:

$$\dot{H}_{solar}(t) = \eta_{coll}\cdot A_{coll}\cdot \dot{G}_T(t), \text{ for all } t, \tag{3}$$

where A_{coll} is the collector area that is assumed to be known, η_{coll} is the collector efficiency, and $\dot{G}_T(t)$ is the total solar irradiance.

2.1.3. Modeling of the CCHP

A CCHP system consists of a gas turbine to meet the electricity demand; an absorption chiller, using high-temperature exhaust gas to satisfy the space cooling demand; and two heat recovery boilers, also using high-temperature exhaust gas to satisfy demands of space heating and domestic hot water [43]. The layout of the CCHP system is sketched inside the bold lines in Fig. 1.

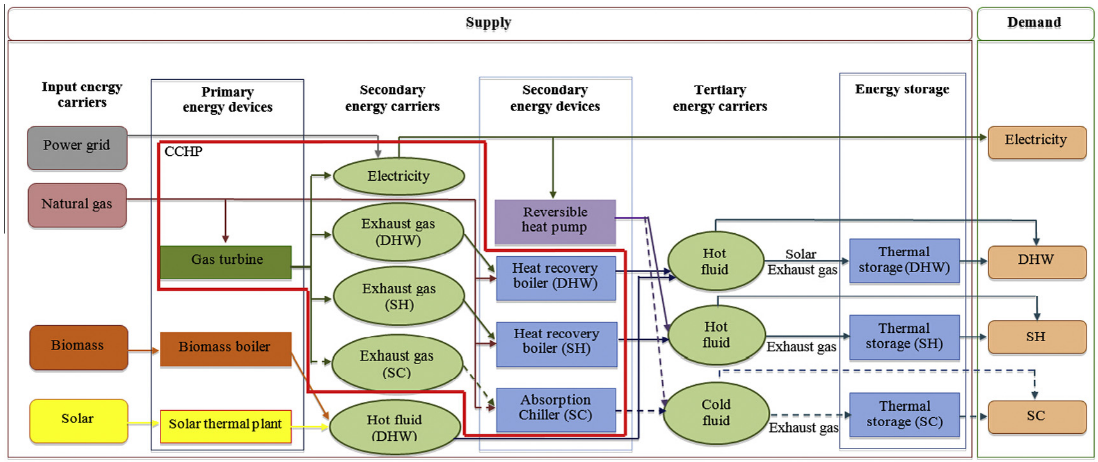

Fig. 1. Scheme of the DES for the operation optimization problem.

Cooling and heating can be also directly generated by supplementary burning of natural gas in the absorption chiller and boilers, respectively. Constraints considered for the CCHP system are presented below.

The CCHP ramp rate constraints limit the variations in the power generation between two successive time steps to be within the ramp-down, DR_{CCHP}, and ramp-up, UR_{CCHP}, [44]:

$$-DR_{CCHP} \leqslant \dot{E}_{CCHP}(t) - \dot{E}_{CCHP}(t-\Delta t) \leqslant UR_{CCHP}, \text{ for all } t, \tag{4}$$

where $\dot{E}_{CCHP}(t)$ and $\dot{E}_{CCHP}(t-\Delta t)$ are energy generation levels at time t and $(t-\Delta t)$, respectively. The ramp-down rate, DR_{CCHP}, and ramp-up rate, UR_{CCHP}, are assumed to be the same [45,46].

The volumetric flow rate of natural gas, $\dot{G}_{GT}(t)$, required by the gas turbine to provide electricity is:

$$\dot{G}_{GT}(t) = \dot{E}_{CCHP}(t)/(\eta_e \cdot LHV_{gas}), \text{ for all } t, \tag{5}$$

where η_e is the turbine gas-to-electric efficiency, that represents how much electricity can be obtained by the combustion of the unit volumetric flow rate of natural gas in the gas turbine, and LHV_{gas} is the lower heat value of natural gas.

The heat rate made available by the exhaust gas recovered from the gas turbine, $\dot{Q}_{GT,ex}(t)$, is:

$$\dot{Q}_{GT,ex}(t) = \dot{E}_{CCHP}(t) \cdot (1-\eta_e-\mu_{GT})/\eta_e, \text{ for all } t, \tag{6}$$

where μ_{GT} is the percent heat loss of the gas turbine which cannot be recovered.

The exhaust gas is subdivided among the absorption chiller and the heat recovery boilers to supply cooling for space cooling, and heating for domestic hot water and space heating. The cooling rate delivered by the exhaust gas to the absorption chiller, $\dot{C}_{ex}(t)$, is:

$$\dot{C}_{ex}(t) = \dot{Q}_{GT,ex}(t) \cdot \xi_{SC}(t) \cdot \eta_{HR,abs} \cdot COP_{abs}, \text{ for all } t, \tag{7}$$

where $\eta_{HR,abs}$ is the waste heat recovery efficiency of the absorption chiller, and COP_{abs} is its coefficient of performance. The continuous decision variable $\xi_{SC}(t)$ is the percentage of exhaust gas supplied to the absorption chiller.

Cooling can be also directly provided by supplementary burning of natural gas in the absorption chiller. The volumetric flow rate of natural gas, $\dot{G}_{abs}(t)$, required by the absorption chiller to directly provide the cooling rate $\dot{C}_{di}(t)$ is:

$$\dot{G}_{abs}(t) = \dot{C}_{di}(t)/(COP_{abs} \cdot \eta_{abs} \cdot LHV_{gas}), \text{ for all } t, \tag{8}$$

where η_{abs} is the efficiency of the absorption chiller combustor.

Therefore, the total generation level of the absorption chiller, $\dot{C}_{CCHP}(t)$, is the sum of the cooling rate obtained by exhaust gas, $\dot{C}_{ex}(t)$, and the cooling rate directly generated by natural gas, $\dot{C}_{di}(t)$:

$$\dot{C}_{CCHP}(t) = \dot{C}_{ex}(t) + \dot{C}_{di}(t), \text{ for all } t. \tag{9}$$

Modeling of heating by the CCHP system for domestic hot water and space heating is similar to that of cooling described above.

The sum of gas turbine exhaust fractions for space cooling, $\xi_{SC}(t)$, in the absorption chiller, for domestic hot water, $\xi_{DHW}(t)$, and for space heating, $\xi_{SH}(t)$, in heat recovery boilers, has to be one, i.e.,

$$\xi_{SC}(t) + \xi_{DHW}(t) + \xi_{SH}(t) = 1, \text{ for all } t. \tag{10}$$

The overall volumetric flow rate of natural gas consumed by the CCHP system, $\dot{G}_{CCHP}(t)$, is:

$$\dot{G}_{CCHP}(t) = \dot{G}_{GT}(t) + \dot{G}_{abs}(t) + \dot{G}^{DHW}_{boil}(t) + \dot{G}^{SH}_{boil}(t), \text{ for all } t. \tag{11}$$

2.1.4. Modeling of the reversible heat pump

A reversible heat pump is used to meet space heating and cooling demands in the heating and cooling modes, respectively. In the heating mode, the electricity consumption of the heat pump, $\dot{E}_{HP}(t)$, to produce the heating rate, $\dot{H}_{HP}(t)$, is given by the following:

$$\dot{E}_{HP}(t) = \dot{H}_{HP}(t)/COP_{HP}, \text{ for all } t, \tag{12}$$

where COP_{HP} is the coefficient of performance of the heat pump in the heating mode. Modeling of cooling mode is similar to that of heating described above.

2.1.5. Modeling of the thermal energy storage systems

The energy stored in the domestic hot water tank at the time t, $H_{sto}(t)$, depends on the non-dissipated energy stored at the previous time step $(t-\Delta t)$; the heat rate input to the storage, $\dot{H}^{in}_{sto}(t)$ (a continuous decision variable); and the heat rate released by the storage, $\dot{H}^{out}_{sto}(t)$ (a continuous decision variable). It can be expressed as follows [35]:

$$H_{sto}(t) = H_{sto}(t-\Delta t) \cdot (1-\varphi_{sto}(\Delta t)) + (\dot{H}^{in}_{sto}(t) - \dot{H}^{out}_{sto}(t)) \cdot \Delta t, \text{ for all } t, \tag{13}$$

where the loss fraction $\varphi_{sto}(\Delta t)$ accounts for the heat losses through the tank walls during the time interval, Δt. Modeling of thermal storage systems for space heating and cooling is similar to that described above.

2.2. Modeling of energy balances

In order to satisfy the given time-varying user demands, electricity and thermal energy balances are formulated by matching supply and demand.

2.2.1. Electricity balance

The electricity rate demand, $\dot{E}_{dem}(t)$, and the electricity rate required by the heat pump, $\dot{E}_{HP}(t)$, must be covered by the sum of the electricity rate delivered by the CCHP system, $\dot{E}_{CCHP}(t)$, and the electricity rate bought from the grid (a continuous decision variable), $\dot{E}_{buy}(t)$, i.e.,

$$\dot{E}_{dem}(t) + \dot{E}_{HP}(t) = \dot{E}_{CCHP}(t) + \dot{E}_{buy}(t), \text{ for all } t. \tag{14}$$

2.2.2. Domestic hot water balance

The heat rate demand for domestic hot water, $\dot{H}^{DHW}_{dem}(t)$, must be satisfied by the sum of the heat rates delivered by the CCHP system (i.e., the sum of the heat rate provided by the exhaust gas and the heat rate directly generated by the natural gas, $\dot{H}^{DHW}_{CCHP}(t)$), the solar thermal plant, $\dot{H}_{solar}(t)$, the biomass boiler, $\dot{H}_{bio}(t)$, and the thermal storage, $\dot{H}^{out}_{sto}(t) - \dot{H}^{in}_{sto}(t)$, i.e.,

$$\dot{H}^{DHW}_{dem}(t) = \dot{H}^{DHW}_{CCHP}(t) + \dot{H}_{solar}(t) + \dot{H}_{bio}(t) + \dot{H}^{out}_{sto}(t) - \dot{H}^{in}_{sto}(t), \text{ for all } t. \tag{15}$$

The space heating and cooling balances can be expressed in a similar way.

2.3. Economic objective

The economic objective is to minimize the total energy cost, *Cost*, which is the sum of three terms: cost of buying electricity from the power grid, cost of natural gas, and cost of biomass as follows:

$$Cost = \sum_t (P_{grid}(t) \cdot \dot{E}_{buy}(t) + P_{gas} \cdot \dot{G}_{buy}(t) + P_{bio} \cdot \dot{B}_{buy}(t)) \cdot \Delta t, \tag{16}$$

where $P_{grid}(t)$ is the time-of-day unit price of electricity from the power grid at time t, P_{gas} and P_{bio} are the constant unit prices of gas and biomass, respectively, and Δt is the length of the time interval. In Eq. (16), the volumetric flow rate of natural gas bought, $\dot{G}_{buy}(t)$, corresponds to the total energy consumption requirement of the CCHP system, and the mass flow rate of biomass bought, $\dot{B}_{buy}(t)$, corresponds to the energy consumption requirement of the biomass boiler.

3. The exergy analysis and the multi-objective optimization method

The exergy analysis and exergetic objective function are discussed in Subsection 3.1. To solve the problem with economic and exergetic objectives, the multi-objective optimization method is discussed in Subsection 3.2.

3.1. Exergy analysis and exergetic objective

In buildings, energy demands are characterized by different energy quality levels. For electrical appliances and lighting, the highest possible quality of energy is needed since electricity is theoretically fully convertible into useful work. The exergy rate required by the building to meet the electricity demand, $\dot{Ex}^{e}_{dem}(t)$, can be evaluated as follows [47]:

$$\dot{Ex}^{e}_{dem}(t) = \dot{E}_{dem}(t), \text{ for all } t. \tag{17}$$

For thermal demands, exergy is directly related to the temperature required for the demand under consideration – the higher temperature required, the higher exergy. The exergy rate required by the building to meet the domestic hot water demand, $\dot{Ex}^{DHW}_{dem}(t)$, can be evaluated as follows [47]:

$$\dot{Ex}^{DHW}_{dem}(t) = F_q(t) \cdot \dot{H}^{DHW}_{dem}(t), \text{ for all } t, \tag{18}$$

with the Carnot factor, $F_q(t)$,

$$F_q(t) = 1 - T_0(t)/T_{req}, \text{ for all } t, \tag{19}$$

which depends on both the temperature required, T_{req}, and the reference temperature, $T_0(t)$. By following a dynamic exergy analysis, the hourly ambient temperatures are considered as reference temperatures [48].

The exergy required by the building to meet the space heating and cooling demands can be evaluated in a similar way.

The total exergy output, Ex_{out}, is the total exergy required to meet the given user energy demands, as formulated in the following:

$$Ex_{out} = \sum_t (\dot{Ex}^{e}_{dem}(t) + \dot{Ex}^{DHW}_{dem}(t) + \dot{Ex}^{SH}_{dem}(t) + \dot{Ex}^{SC}_{dem}(t)) \cdot \Delta t. \tag{20}$$

At the supply side, input energy carriers are characterized by different energy quality levels as well. Instead of analyzing the exergy input and output of each step in the energy supply chain from generation to utilization, the total exergy input to DES and the total exergy output required to meet the energy demands are considered for simplicity, assuming known the efficiencies of energy devices. The energy carriers input to the DES under consideration include electricity, natural gas, biomass and solar, as discussed in the following.

Electricity from the power grid is an energy carrier provided by power generation plants, and their exergy efficiency, ε_{gen}, is based on the technologies used in the plants. The exergy rate of the electricity from the power grid is [36,37]:

$$\dot{Ex}_e(t) = \dot{E}_{buy}(t)/\varepsilon_{gen}, \text{ for all } t. \tag{21}$$

For natural gas, its specific chemical exergy is the maximum work that can be obtained from the substance, by taking it to the chemical equilibrium with the reference environment at the constant temperature and pressure [6]. The exergy input rate of natural gas, $\dot{Ex}_{gas}(t)$, is the exergy input to the CCHP system, and it is the overall natural gas volumetric flow rate consumed by the CCHP system, $\dot{G}_{CCHP}(t)$, multiplied by the specific chemical exergy of natural gas, ex_{gas}, i.e.,

$$\dot{Ex}_{gas}(t) = ex_{gas} \cdot \dot{G}_{CCHP}(t), \text{ for all } t. \tag{22}$$

The specific chemical exergy of natural gas, ex_{gas}, can be evaluated by multiplying the exergy factor, ς_{gas}, and the lower heat value, LHV_{gas},

$$ex_{gas} = \varsigma_{gas} \cdot LHV_{gas}. \tag{23}$$

According to [6], the exergy factor for natural gas is equal to 1.04 ± 0.5%.

Similar to that of natural gas, the exergy input rate of the biomass fuel, $\dot{Ex}_{bio}(t)$, is the exergy input rate to the biomass boiler. It is the product of the biomass mass flow rate consumed by the biomass boiler, $\dot{B}_{boil}(t)$, and the specific chemical exergy of biomass, ex_{bio}, i.e.,

$$\dot{Ex}_{bio}(t) = ex_{bio} \cdot \dot{B}_{boil}(t), \text{ for all } t. \tag{24}$$

The specific chemical exergy of biomass, ex_{bio}, can be evaluated as the product of the exergy factor, ς_{bio}, and the lower heat value, LHV_{bio},

$$ex_{bio} = \varsigma_{bio} \cdot LHV_{bio}. \tag{25}$$

According to [6], the values of the exergy factor for wood are in the range 1.15–1.30.

Solar energy from the collectors is considered as a low-exergy source since the solar exergy input rate, $\dot{E}x_{solar}(t)$, is evaluated at the output of the solar collector field [49,50], i.e.,

$$\dot{E}x_{solar}(t) = \dot{H}_{solar}(t) \cdot (1 - T_0(t)/T_{coll}^{out}), \text{ for all } t, \tag{26}$$

where T_{coll}^{out} is the temperature of the heat transfer fluid at the exit of the collector.

The total primary exergy input, Ex_{in}, is formulated as the sum of the exergy rates of the primary energy carriers over time, as follows:

$$Ex_{in} = \sum_t (\dot{E}x_e(t) + \dot{E}x_{gas}(t) + \dot{E}x_{bio}(t) + \dot{E}x_{solar}(t)) \cdot \Delta t. \tag{27}$$

With the exergy output and input defined above, the overall exergy efficiency is the ratio of the total exergy output, Ex_{out}, to the total primary exergy input, Ex_{in}, as follows:

$$\psi = Ex_{out}/Ex_{in}. \tag{28}$$

As mentioned earlier, the total exergy required to meet the given energy demands is known, and the overall exergy efficiency in Eq. (28) can be increased by reducing the exergy input to the DES. Therefore, the exergetic objective is formulated as the total primary exergy input, Ex_{in}, as in Eq. (27).

3.2. Multi-objective optimization method

With the exergetic objective function formulated in Eq. (27) and the economic objective function formulated in Eq. (16), the problem has two objective functions to be minimized. To solve this multiple-objective problem, a single objective function is formulated as a weighted sum of the total energy cost, *Cost*, and the total primary exergy input, Ex_{in}:

$$F_{obj} = c \cdot \omega \cdot Cost + (1 - \omega) \cdot Ex_{in}, \tag{29}$$

where the constant c is chosen such that the terms $c \cdot Cost$ and Ex_{in} have the same order of magnitude. The Pareto frontier involving the best possible trade-offs between the two objectives can be found by varying the weight ω in the interval 0–1. The solution that minimizes the total energy cost is obtained for $\omega = 1$, whereas the solution that minimizes the total exergy input (i.e., maximizes the overall exergy efficiency) is obtained for $\omega = 0$. Then the constant c is calculated as the ratio of the total exergy input obtained by energy cost minimization to the total cost obtained by exergy input minimization. With constant c, the best possible trade-offs between the two objectives, appertaining to the Pareto frontier, are obtained by solving the problem with values of ω varying in-between 0 and 1. The problem formulated in Sections 2 and 3 is linear and involves both discrete and continues variables, so this mixed integer linear programming problem is to be solved by branch-and-cut. Mixed-integer linear programming problems are usually difficult to solve because a set of decision variables are restricted to integer values. Branch-and-cut is generally powerful for mixed-integer linear optimization problems. In the method, all integrality requirements on variables are first relaxed, and the relaxed problem can be efficiently solved by using a linear programming method. If the values of all integer decision variables turn out to be integers, the solution of the relaxed problem is optimal to the original problem. If not, the convex hull (the smallest convex set that contains all feasible integer solutions in the Euclidean space) is needed since once it is obtained, all integer decision variables of the linear programming solution are integers and optimal to the original problem. The process of obtaining the convex hull, however, is problem dependent, and can itself be NP hard. Valid cuts that do not cut off any feasible integer solutions are added, trying to obtain the convex hull first. If the convex hull cannot be obtained, low-efficient branching operations may then be needed on the variables whose values in the optimal relaxed solution violate their integrality requirements. The objective value of the current optimal relaxed solution is a lower bound, and can be used to quantify the quality of a feasible solution. The optimization stops when CPU time reaches the pre-set stop time or the relative gap falls below the pre-set stop gap.

4. Numerical testing

The method developed above has been implemented by using IBM ILOG CPLEX Optimization Studio Version 12.5. Branch-and-cut is powerful for mixed-integer linear optimization problems, and easy to code by using commercial solvers. CPLEX, a popular and powerful solver where branch-and-cut is implemented with flexibility and high-performance, is therefore used to solve the optimization problem. Two examples are presented. The first, a textbook example, shows that the optimized operation of the DES allows reducing energy costs and primary exergy input, compared with conventional energy supply systems. In the second example, the targeted energy consumer is a large hotel. The Pareto frontier involving the best possible trade-offs between the economic and the exergetic objectives is presented, and the operation strategies of the DES under different weights for the two objectives are discussed. Then, the contribution of each energy device in reducing energy costs and primary exergy input is analyzed. The effects of the constant efficiency assumption on the optimized operation strategies attained by the multi-objective optimization are also analyzed.

4.1. Example 1

In this example, a building located in Beijing is considered, and two types of energy demands are involved, electricity and space heating, with different energy quality levels required. Two configurations of the energy supply system under consideration are described in Fig. 2. The first is a conventional one with only the grid power to meet both the electricity demand directly and the electricity required by an electric heater (100% energy conversion efficiency) to satisfy the space heating demand. The electricity balance formulated in (14) needs to be modified as follows:

$$\dot{E}_{dem}(t) + \dot{E}_{EH}(t) = \dot{E}_{buy}(t), \text{ for all } t, \tag{30}$$

where $\dot{E}_{EH}(t)$ represents the electricity rate required by the electric heater. The second configuration is a DES involving a CCHP system and the power grid. The heat pump related term in the electricity balance (14) needs to be deleted.

To evaluate the exergy required by the building to meet the space heating demand, the indoor air temperature is set to 293.15 K. The ambient temperature, 269.15 K, is assumed as the reference temperature. Two non-consecutive hours are chosen. Energy prices as well as energy rate demands and exergy required to satisfy these energy demands for a typical winter day in January are presented in Table 1.

In the first configuration, the building demands are completely satisfied by the grid power, therefore there is no trade-off between the energy cost and exergy efficiency. For the two hours under consideration, the total energy cost is $ 30.45 and the total exergy input is 546.88 kJ with an 11.9% overall exergy efficiency. For the second configuration, there are several operation strategies to meet the building demands. The Pareto frontier consisting of a set of possible trade-offs between the two objective functions (i.e., *Cost* and Ex_{in}) is presented in Fig. 3, and the overall exergy

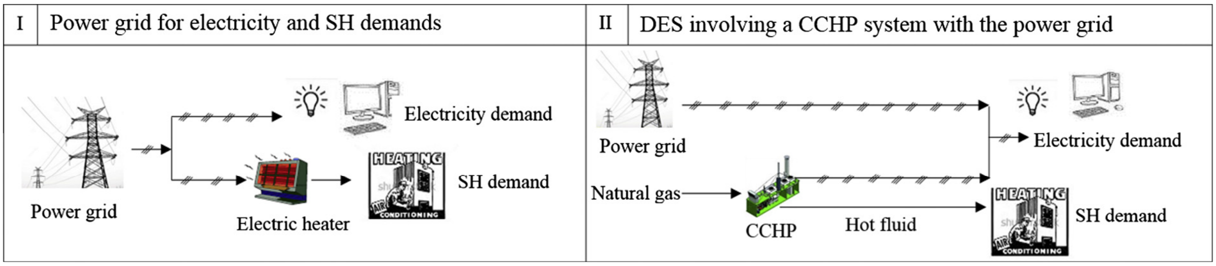

Fig. 2. Configurations analyzed to meet the energy demands of a building in Beijing.

Table 1
Energy prices, energy and exergy rate demands.

Hour		1	2
Energy price	Power grid price ($/kW h)	0.07	0.20
	Gas price ($/Nm^3)	0.38	0.38
Energy rate demand	Electricity (kW)	5	50
	Space heating (kW)	30	90
Exergy rate demand	Electricity (kW)	5	50
	Space heating (kW)	2.5	7.4

efficiency ψ is also presented. The point marked with *a* is obtained by minimizing the total energy cost. The electricity demand is satisfied by the grid power in the first hour since its price is low, and satisfied by CCHP in the second hour in view of the higher grid price. It can be seen that when the economic objective function is minimized, the operation of the DES is sensitive to the grid price. At this point, the total energy cost is $ 9.64, and it is reduced by nearly 70% as compared with that of the first configuration because of the usage of the CCHP system to take advantage of the grid price variation. The point marked with *b* is obtained by minimizing the total exergy input. In the first hour, the electricity demand is completely satisfied by the CCHP system despite of low grid power price, and the space heating demand is satisfied by the exhaust heat and the direct burning of natural gas in the boiler since the exhaust heat is not enough to cover the demand. In the second hour, 43.87 kW of the demand is satisfied by the CCHP system such that the space heating demand is satisfied by the exhaust heat without waste. When the exergetic objective function is minimized, the operation of the DES is independent of the grid power price variation. The total exergy input is 246.23 kJ, and it is reduced by about 55% as compared with that of the first configuration by the usage of exhaust gas in the CCHP system. This example shows that the energy cost and input exergy are sensitive to the variation of the DES operation.

4.2. Example 2

In this example, the targeted system is a hypothetic large hotel in Beijing with a 30,000 m^2 area, with the power grid, natural gas,

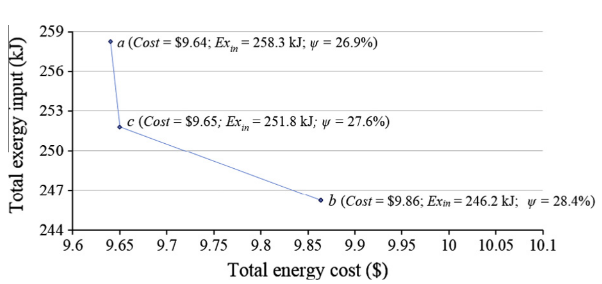

Fig. 3. Trade-offs between the two objective functions for the second configuration.

biomass, and solar energy as primary energy carriers. Electricity, domestic hot water, space heating and cooling demands are considered, with different energy quality levels required. A typical winter day of January and a typical summer day of July are chosen with one hour as time-step. The configuration of the DES analyzed, including the sizes of energy devices, is shown in Fig. 4.

In the following, the input data for the optimization model are described in Subsection 4.2.1. The Pareto frontiers for both winter and summer cases are presented in Subsection 4.2.2. The optimized operation of the DES is also discussed for a trade-off point on the Pareto frontier to show how the operation strategy affects the energy costs and input exergy under different weights for the two objectives. To show how each energy device contributes to the reduction of energy costs and exergy input, results of energy cost minimization and exergy input minimization are presented for different DES configurations in Subsection 4.2.3. To show how the constant efficiency assumption affects the optimized operation strategies, the performance of the heat pump and the variation of the gas turbine electric efficiency at partial loads are considered in the multi-objective optimization in Subsection 4.2.4.

4.2.1. Input data

The required input data include building energy demands, prices and exergy factors of primary energy carriers, and efficiencies of energy devices as discussed below.

4.2.1.1. Building energy demands. The hourly electricity, domestic hot water, space heating and cooling demands are taken from a comprehensive investigation about energy demands of hotels in Beijing [42], and the energy rate demand profiles for a typical winter day of January and of July, respectively, are chosen as shown in Fig. 5. The exergy of thermal demands for each day is evaluated by assuming the reference temperatures as the hourly ambient temperatures of the corresponding day, taken from meteorological data in Beijing [51]. The temperatures required for domestic hot water, space heating and cooling demands, T_{req}, are set to be 333.15 K, 293.15 K and 299.15 K, respectively [52].

4.2.1.2. Prices and exergy of primary energy carriers. As mentioned earlier, power grid, natural gas, biomass, and solar energy, are primary energy carriers. The first three are assumed unlimited in this study, for simplicity. The grid power price is time-varying as shown in Fig. 5 [53], and the exergy efficiency of the power generation plant is assumed equal to 0.32 [54], a typical value when electricity is mostly generated by coal-fired thermal power plants as in China [55]. The price of natural gas is assumed equal to 0.38 $/Nm^3 [53], and the fuel of the biomass boiler is assumed to be wood pellet with a price of 70 $/t [56]. Their exergy factors are assumed equal to 1.04 and 1.16 [6], respectively. To evaluate the heat rate provided by the collector field, for each hour of the representative winter day of January, the solar irradiance has been evaluated as the average of the hourly mean values of the solar irradiance in the corresponding hour of all January days. The same

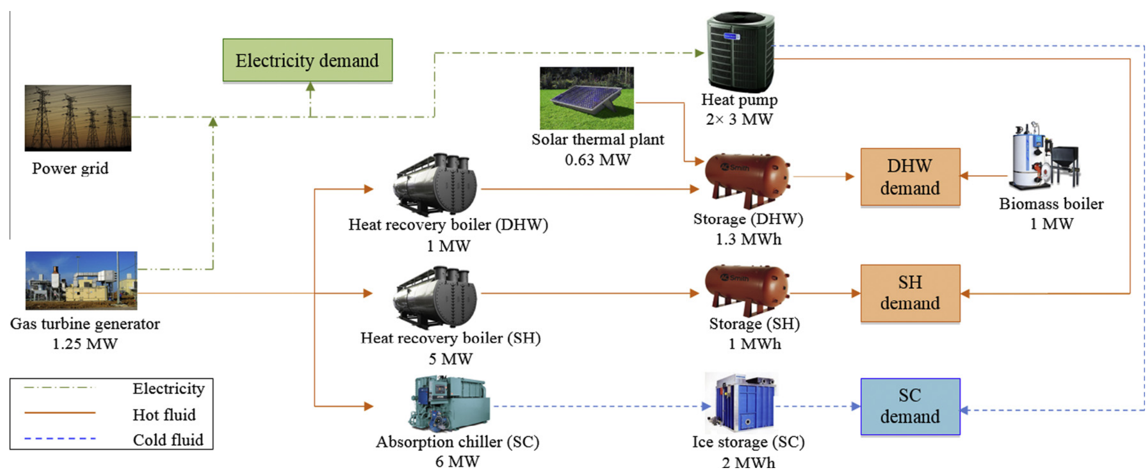

Fig. 4. DES configuration analyzed in Example 2 for the hypothetical hotel in Beijing.

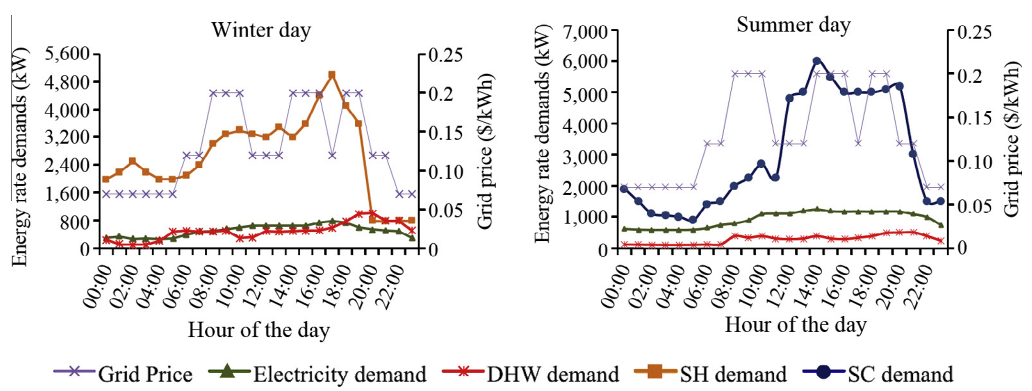

Fig. 5. Energy rate demands of a hypothetic hotel in Beijing and grid price.

has been done for a representative summer day of July [51]. In the evaluation of the Carnot factor for the solar exergy input rate (Eq. (19)), the temperature of the heat transfer fluid at the exit of the collector field is assumed constant and equal to 353.15 K.

4.2.1.3. Efficiency of energy devices and thermal storages. In the following reference is made to a turbine with an actual nominal peak output of 1250 kW and an exhaust gas temperature of 785.15 K. It operates at a 24% gas-to-electric turbine efficiency with an 8% heat loss efficiency [57]. A gas fired absorption chiller that can be indirectly fired by turbine exhaust gas is chosen for the system. The COP of the chiller unit is 1.2 with an exhaust gas temperature of 443.15 K and its combustion efficiency is 85% [58]. An efficiency of 90% is chosen for the natural gas boiler. The exhaust gas temperature of the heat recovery boiler can be safely brought down to 403.15 K. The heat recovery efficiency of the boiler is defined as the ratio of difference between the initial exhaust gas temperature from the turbine and the final exhaust gas temperature out of the heat recovery boiler to the difference between the initial exhaust gas temperature from the turbine and the ambient temperature. The heat recovery efficiency of the absorption chiller is determined in the same way. The efficiencies of the wood pellet biomass boiler and solar thermal are assumed to be 80% and 40%, respectively. Typical values of the coefficient of performance of heat pumps in Beijing have been used. The loss fractions of thermal storages have been assumed equal to 0.10. The above mentioned data are listed in Table 2.

4.2.2. Pareto frontier

The optimization problem can be solved within several seconds with a mixed integer gap 0.1%, and the Pareto frontiers of both winter and summer cases are shown in Fig. 6. For the winter case, the point marked with *a* is obtained by minimizing the total daily energy cost, and the daily energy cost is 3340 $/d whereas the daily exergy input is 100,210 kJ/d. The point marked with *b* is obtained by minimizing the total daily exergy input. The daily energy cost is 3549 $/d whereas the daily exergy input is 92,548 kJ/d. The points between the extreme points are found by subdividing the

Table 2
Efficiencies of energy devices and thermal storage systems.

Primary energy devices	Efficiency	
	Electrical	Thermal
Gas turbine	0.24	0.68
Biomass boiler		0.80
Solar thermal		0.40
Secondary energy devices	Efficiency	
	Heating mode	Cooling mode
Heat pump	$COP = 3.0$	$COP = 3.2$
Heat recovery boiler	$\eta_{boil} = 0.90$ $\eta_{HR,boil} = 0.74$	
Absorption chiller		$COP_{abs} = 1.2$ $\eta_{abs} = 0.85$ $\eta_{HR,abs} = 0.70$
Thermal storages loss fraction:	$\varphi_{sto} = 0.10$	

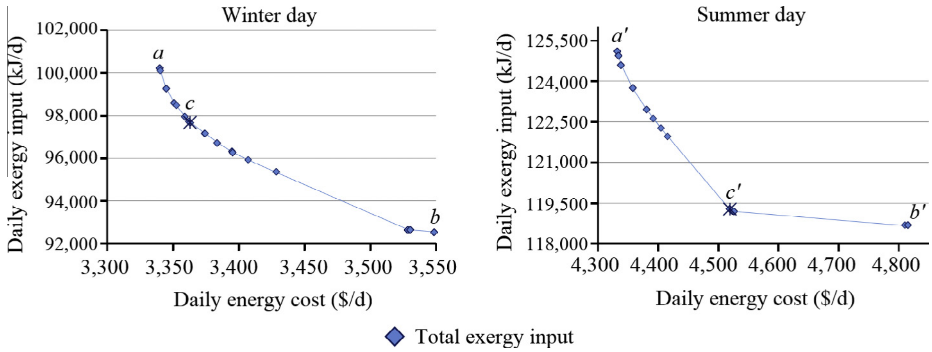

Fig. 6. Trade-offs between the two objective functions.

weight interval into 100 equally-spaced points. There are 17 points since some solutions have been found under more than one weight values. For the summer case, its Pareto frontier with 13 points is obtained in the same way, where the points marked with *a*′ and *b*′ are obtained by minimizing the total daily energy cost and the total daily exergy input, respectively. The operators of the DES can choose the operation strategy from the Pareto frontier based on their cost and exergy preference and priorities. For the illustration purpose, the point marked with *c* in the winter case is chosen to show the optimized operation of the DES under a higher weight of 0.7 for the economic objective. The point marked with *c*’ in the summer case is chosen to show the optimized operation of the DES under a higher weight of 0.62 for the exergetic objective.

Fig. 7 shows the hourly grid power price, electricity rate demand, electricity rate consumed by the heat pump, electricity rate provided by the CCHP system, and electricity rate bought from the power grid, for point *c* of the winter day and point *c*’ of the summer day. In the winter case, electricity is bought from the power grid when its price is low, e.g., from 0:00 to 5:00, and it is used to meet the electricity demand and to drive the heat pump. Conversely, when the grid power price increases, the CCHP system is used to meet the electricity demand and to drive the heat pump, for example, at 15:00, 16:00, 18:00 and 19:00. In the summer case, the operation of the DES is less sensitive to the grid power price variation. For instance, from 0:00 to 5:00, despite the low grid power price, electricity from the CCHP system is mostly used to meet the electricity demand and to drive the heat pump. With less electricity bought from the power grid, the total daily exergy input would be lower.

The hourly domestic hot water rate demand, the hourly heat rates provided by the CCHP system, by the biomass boiler, by the solar thermal, and the thermal energy stored, are reported in Fig. 8. The figure points out the differences in the operation of the DES under different weights for the economic and exergetic objectives. For point *c* in the winter case, the biomass boiler, instead of the gas-fired boiler, is used to meet the domestic hot water demand, because of its lower price. In addition, since the solar thermal plant is sized to almost totally satisfy the hot water demand in the winter day during the insolation hours, thermal energy is never stored during the insolation hours. Conversely, for point *c*’ in the summer case, the biomass boiler is never used to meet the domestic hot water demand. This is due to the fact that biomass is a high-quality renewable energy resource, and it should not be used for the low quality thermal demand. This result agrees with those presented in [1], where different energy supply systems for space heating and domestic hot water demands (i.e., natural gas boiler, wood pellet boiler, ground source heat pump, and waste district heat), were compared through exergy analysis. It was shown that the exergy input of the wood-fuelled boiler is the largest among the four options, since wood is a renewable and high quality energy resource, but the conversion efficiencies of wood boilers are usually not as high as those of conventional natural gas boilers. The fact that the exergy input is the largest indicates that such an energy supply does not promote efficient use of the potential of the energy sources used. In addition, in the summer case, thermal energy is mostly stored during the insolation hours because of the higher solar irradiation and the lower hot water demand, and the stored energy is recovered for the evening hours.

The hourly grid prices, hourly space heating and cooling rate demands, hourly heat and cooling rates provided by the CCHP system and by the heat pump, and thermal energy stored, are reported in Fig. 9. Results are similar to those shown in Fig. 8. In the winter case, the operation of the DES is more sensitive to the grid price variation, and in the summer case, the operation of the DES is less sensitive to that.

4.2.3. Energy cost and exergy input for various configurations of the DES

To show how each energy device contributes to the reduction of energy costs and exergy input, various configurations of the DES to meet the building demands for the winter day are now analyzed. For each configuration, one energy device is taken out of the DES, including the biomass boiler, thermal storage system, the solar thermal plant, the heat pump, the gas turbine in the CCHP system, and the entire CCHP system. The total daily energy cost and exergy input obtained by minimizing the energy cost and exergy input, as well as the conventional system, i.e., all from the grid power, are compared in Fig. 10. Results for the summer day are similar.

Configuration 1 is the reference case, consisting of all energy devices mentioned in Section 2. Configuration 2 excludes the biomass boiler from the reference case. When the total energy cost is minimized, results show a higher total daily energy cost than that of the reference case, due to the low price of biomass. When the exergy input is minimized, the daily energy cost and exergy input are the same as those in the reference case since the biomass boiler is not used to meet the low-quality domestic hot water demand. This is due to the fact that biomass is a high-quality renewable energy resource, and should be used to supply high exergy demands such as electricity. This result agrees with those presented in [18], where it was shown that when the biomass is used as fuel of boilers for thermal purposes, a lower exergy efficiency is attained as compared with when the biomass is used as fuel of CHP plants. Minimization of not only fossil but also renewable energy input promotes efficient use of all energy resources.

Configuration 3 excludes the thermal energy storage from the reference case. When the economic objective function is minimized, the total daily energy cost is higher than that of the reference case. When the exergetic objective function is minimized, the total daily exergy input is higher than that of the reference case. This confirms that the use of thermal storage systems

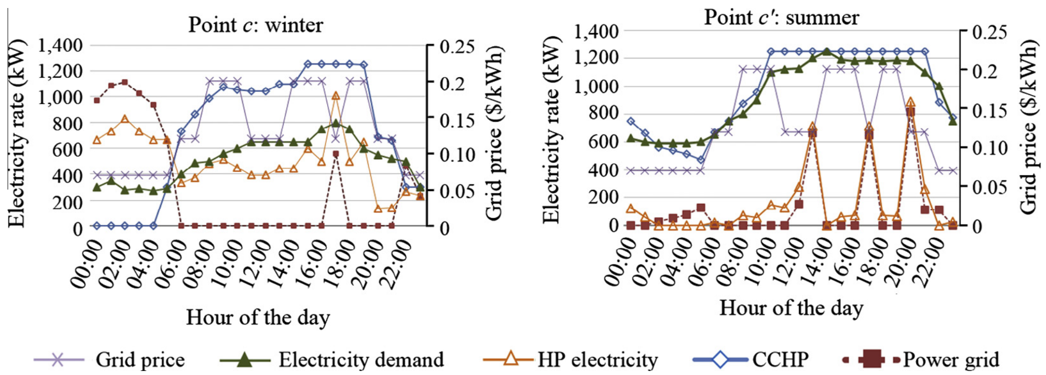

Fig. 7. Hourly grid price, electricity rate demand, electricity rate consumed by the heat pump, electricity rates provided by the CCHP and the power grid, for points *c* and *c*′.

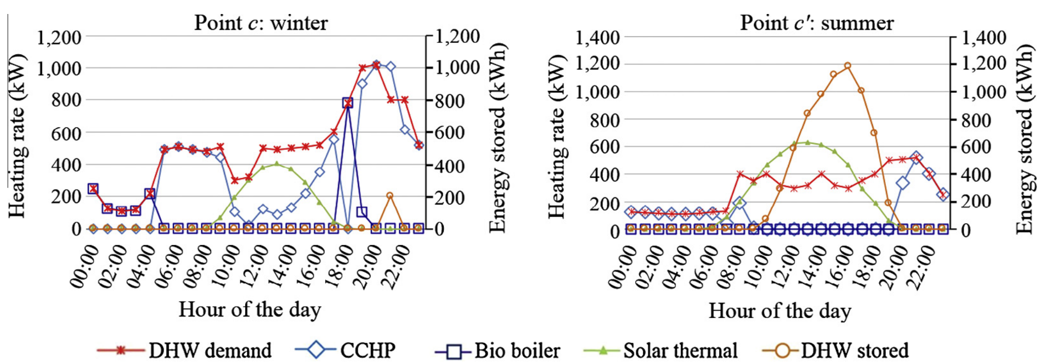

Fig. 8. Hourly domestic hot water rate demand, hourly heat rates provided by CCHP, biomass boiler, solar thermal plant, thermal energy stored, for points *c* and *c*′.

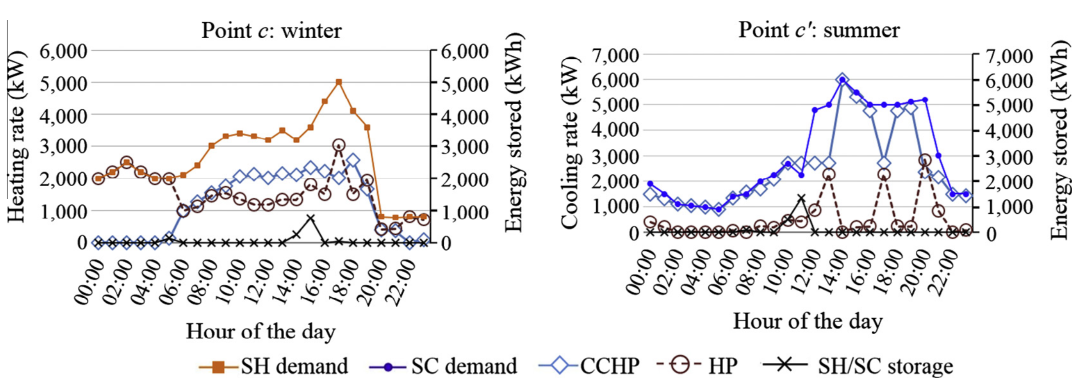

Fig. 9. Hourly space heating/cooling rate demands, hourly heat/cooling rates provided by the CCHP system and by the heat pump, thermal energy stored, for points *c* and *c*′.

increases economic savings and improves the efficiency of energy resource use.

Configuration 4 excludes the solar thermal plant, and the results are similar to those for Configuration 3. In the reference case, the solar thermal plant is used to meet the low-quality domestic hot water demand. When the solar thermal plant is excluded, other energy devices are used to meet the domestic hot water demand with a higher total exergy input. The absence of the free solar energy resource also increases the energy costs. For Configuration 5, the significant increase in the energy cost and input exergy when the heat pump is excluded demonstrates the essential role of the heat pump because of its high conversion efficiency.

Configuration 6 excludes the gas turbine generator of the CCHP system. Without exhaust gas, the heat recovery boilers and the absorption chiller are driven by natural gas. Results underline the important role of the gas turbine in the reduction of both the energy cost and exergy input. When the energy cost is minimized, the increase in the cost is mainly due to the fact that the electricity demand is now fully satisfied by the grid power even when its price is high. When the exergy input is minimized, the domestic hot water demand is satisfied by the gas-fired boiler during non-insolation hours while the biomass boiler is not used although it is cheaper than natural gas. Both wood and natural gas are high-quality energy resources, but the efficiency of the biomass boiler is lower than that of the conventional gas-fired boiler. Configuration 7 excludes the entire CCHP system. Results show that the total energy cost as well as the total exergy input are the same for both energy cost and exergy input minimization, implying that the total energy costs and exergy input are the same

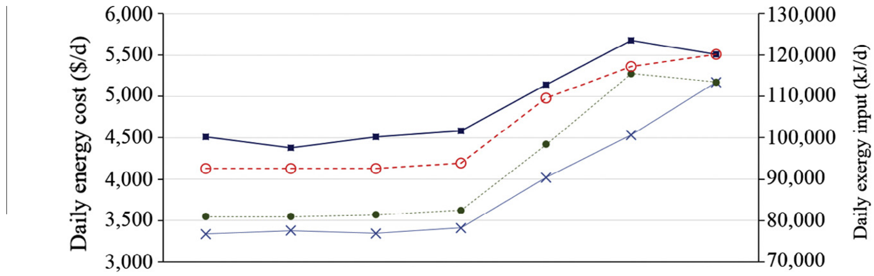

	1)All	2)No Bio boil	3)No storage	4)No ST	5)No HP	6)No GT	7)No CCHP	All from grid
Cost ($\omega = 1$)	3,339.7	3,378.7	3,345.5	3,410.5	4,021.9	4,533.4	5,174.3	12,728
Cost ($\omega = 0$)	3,548.6	3,548.6	3,569.6	3,623.6	4,419.5	5,277.1	5,174.3	12,728
Ex ($\omega = 1$)	100,210	97,581	100,240	101,720	112,850	123,500	120,240	277,291
Ex ($\omega = 0$)	92,548	92,548	92,615	93,915	109,550	117,240	120,240	277,291

Fig. 10. Daily energy cost and exergy input for Configurations 1–7 and the conventional system in the winter day.

for all weights because there are other no choices to meet energy demands. The cost is higher than that of Configuration 6 under cost minimization, since space heating is fully satisfied by the heat pump driven by electricity from the power grid. The daily exergy input is larger than that in Configuration 6 under exergy minimization, because of the high exergy content of the electricity bought from the power grid. The exergy increase is also because of the use of the biomass boiler to meet the domestic hot water demand.

Results found in this work, related to the usefulness of solar thermal, heat pumps and waste heat recovery from an exergy perspective, agree with those presented in [19,20]. In [19], four options (i.e., heat pump, condensing boiler, conventional boiler and solar collector) were analyzed and compared to meet the space heating demand of a building through energy and exergy analysis, and it was shown that the heat pump and the solar thermal collectors have the best performance in terms of exergy efficiency. In [20], it was shown that, among different energy supply systems for heating and cooling purposes, the highest overall exergy efficiencies are achieved by solutions employing waste heat from a cogeneration plant, followed by highly efficient electrical heat pumps.

Finally, the daily energy cost and exergy input are evaluated for the conventional energy supply system. The grid power is used to meet the electricity demand directly and the electricity required by an electric heater (100% energy conversion efficiency) and by an electric boiler (98% energy conversion efficiency) to satisfy the space heating and domestic hot water demands, respectively. With all demands satisfied by the grid power, the total energy cost is 12,728 $/d, and it is 3.8 times of the cost for the reference case (3340 $/d) obtained by the cost minimization. While the total exergy input is 277,291 kJ/d, and it is nearly 3 times of the exergy for the reference case (92,548 kJ/d) obtained by the exergy input minimization. It can be seen that by the optimized operation of the DES, the energy cost and exergy input are much reduced.

4.2.4. Effect of partial loads performance of heat pump and gas turbine in the CCHP system on the optimized operation strategies of the DES

To show how the constant efficiency assumption affects the optimized operation strategies of the DES, while maintaining the problem linearity, the performance of the heat pump and the gas turbine in the CCHP system at partial loads is analyzed for the winter case in this subsection. The CCHP system and the heat pump are the two energy devices which contribute to the reduction of energy costs and primary exergy input in a major way, as shown in Subsection 4.2.3.

Unlike the other energy devices, the partial load performance of the heat pump can be deduced from the full load value [59] and the problem linearity is maintained. However, the electric efficiency of the gas turbine generator is a nonlinear function of the generation level (a continuous decision variable), which makes the problem nonlinear. Therefore, to maintain the problem linear, the effects of the variation of the gas turbine electric efficiency at partial loads on the optimized operation strategies of the DES are evaluated through a heuristic iterative approach. This approach consists of iterating the following steps till convergence.

(1) Solve the optimization problem including the partial load performance of the heat pump and considering the turbine electric efficiency as a vector of 24 components.
(2) For each hour of the day, evaluate the gas turbine electric efficiency from the gas turbine efficiency-load curve [60] by entering the curve with the electricity provided by the gas turbine coming from step 1, expressed in percentage of the full load.
(3) If convergence is not reached, update the turbine electric efficiency vector, and then return to step 1.

At the beginning, step 1 has to be performed considering for all 24 h the gas turbine electric efficiency equal to the one at full load.

Accounting for the performance of the heat pump and the variation of the gas turbine electric efficiency at partial loads, under cost minimization, the daily energy cost increases by 2.7% as compared with the minimum energy cost obtained with constant efficiencies of all the energy devices. Under exergy minimization, the daily primary exergy input increases by 2.5% as compared with the minimum primary exergy input obtained with constant efficiencies of all the energy devices.

The optimized operation strategies (shares of the energy provided by each energy device normalized on the total energy provided to meet the corresponding energy demand in the winter day), under different weight values, are compared in the following. Results for the summer case are similar. Figs. 11 and 12 show the optimized operation strategies to meet the electricity load (sum of the electricity demand and electricity required by the heat pump) and thermal demands, respectively, obtained by varying the weight ω from 0 to 1 with a 0.1 increase: (a) considering constant efficiencies for all the energy devices, (b) considering the performance of the heat pump and the variation of the gas turbine electric efficiency at partial loads, while maintaining constant efficiencies of the other energy devices. From the comparison between (a) and (b) of the two figures, it can be seen that the trends of the operation strategies are almost the same when ω varies from 1 to 0 (from economic to exergetic optimization).

Fig. 11 shows that for both the cases, when ω varies from 1 to 0, the share of the electricity provided by the CCHP system increases, highlighting the importance of this energy device for the exergetic optimization. However, the CCHP system is less used when the

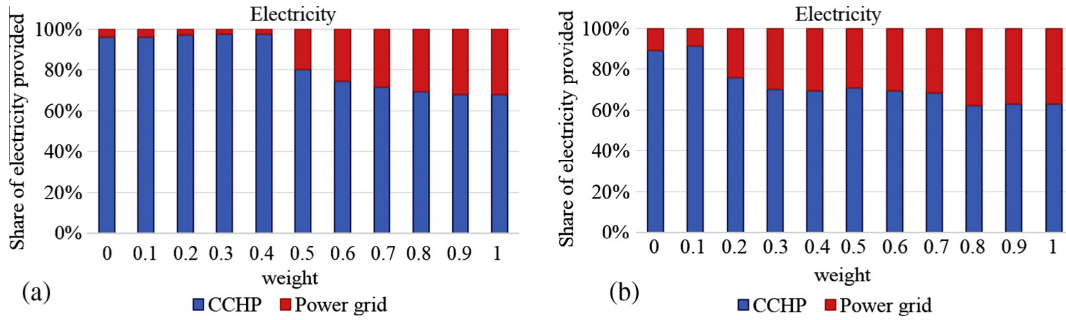

Fig. 11. Share of electricity provided by CCHP system and power grid in the winter day: (a) Considering constant efficiencies of all the energy devices; (b) Considering the performance of the heat pump and the variation of the gas turbine electric efficiency at partial loads and constant efficiencies of other energy devices.

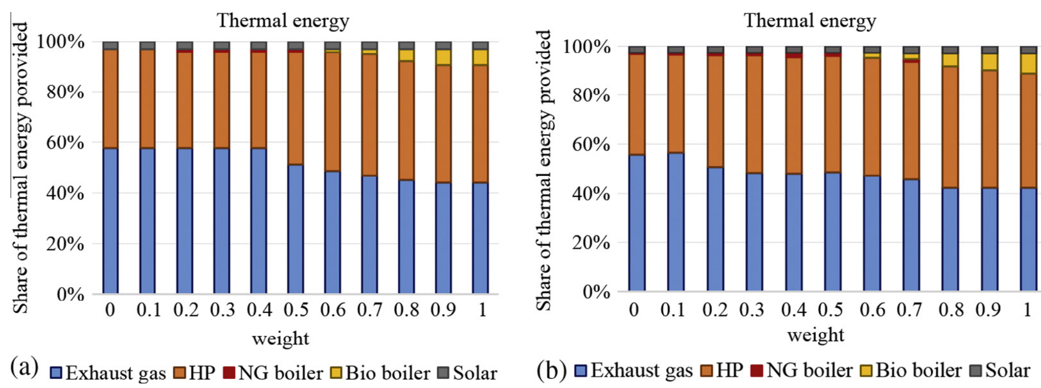

Fig. 12. Share of thermal energy provided by energy devices in the DES in the winter day: (a) Considering constant efficiencies of all the energy devices; (b) Considering the performance of the heat pump and the variation of the gas turbine electric efficiency at partial loads and constant efficiencies of other energy devices.

performance of the heat pump and the variation of the gas turbine electric efficiency at partial loads are taken into account. In this case, the CCHP system is mostly used at high loads, since its electric efficiency reduces at low loads. Conversely, when a constant efficiency is assumed, the CCHP system is used also at lower loads, resulting in the higher use of the CCHP system and the lower use of grid power, as shown in Fig. 11a. The share of the electricity provided by the power grid is generally slightly higher when the performance of the heat pump and the variation of the gas turbine electric efficiency at partial loads are taken into account. In this case, the heat pump is mainly off or operates at full load, since its efficiency is the highest under full load condition. Conversely, if a constant efficiency is assumed, the heat pump is used mostly at partial loads, resulting in the higher use of the CCHP system and the lower use of grid power, as shown in Fig. 11a.

Fig. 12 shows that for both the cases, when ω varies from 1 to 0, the use of exhaust gas for thermal purposes increases, coherent with the increasing use of CCHP, highlighting the importance of waste heat recovery for the exergetic purpose. In addition, the use of the heat pump slightly reduces, showing that the heat pump is important for both the objectives, and its contribution in reducing energy costs is higher than that in reducing primary exergy input. Also the use of the biomass boiler reduces, highlighting the importance of this energy device for energy costs. However, when the performance of the heat pump and the variation of the gas turbine electric efficiency at partial loads are taken into account, the use of the exhaust gas for thermal purposes is slightly lower, coherent with the lower use of CCHP system. Conversely, the use of the heat pump is slightly higher when the performance of the heat pump at partial loads is considered, since in this case the heat pump is off or it is used at full load with the maximum efficiency.

5. Conclusions

In this paper, exergy modeling and optimization are used for the operation of a DES involving several energy devices that convert a set of primary energy carriers to meet given time-varying demands with different energy quality levels. The Pareto frontier, consisting of the best possible trade-offs between the energy cost and exergy efficiency, is obtained by minimizing a weighted sum of the economic and exergetic objectives using branch-and-cut. Results show that the operation of the DES is sensitive to the weights for the two objectives. In addition, the contributions of each energy device in reducing energy costs and the total exergy input are demonstrated, showing that both fossil and renewable energy, when appropriately combined, significantly reduce the energy cost and improve the exergy efficiency. Finally, the performance of the heat pump and the variation of the gas turbine electric efficiency at partial loads are considered in the multi-objective optimization. Slight variations in the optimized operation strategies of the DES are found, as compared to those obtained under the assumption of constant efficiency of all the energy devices. For the DES considered, under cost minimization the daily energy cost increases by 2.7% and under exergy minimization the daily primary exergy input increases by 2.5%, as compared with values obtained with the constant efficiency assumption for all the energy devices.

Although the capital investment costs of DESs are generally high as compared with conventional energy supply systems using the grid power only, it is shown that the energy costs can be much reduced and the overall exergy efficiencies can be significantly improved by the optimized operation of DESs. The operators of DESs can choose the operation strategy from the Pareto frontier based on costs, essential in the short run, and sustainability, crucial in the long run. Although there are no benchmarks about exergy efficiency yet, results demonstrate that exergy should be included in the energy legislation to improve sustainability by rational use of various energy resources.

Acknowledgement

Authors thank the Università di Napoli Federico II for funding this study within the agreement with the University of Connecticut and the Smart grid con sistemi di poligenerazione distribuita (Poligrid).

References

[1] ECBCS – Annex 49 – Low Exergy Systems for High Performance Buildings and Communities, homepage. Available <http://www.ecbcs.org/annexes/annex49.htm> [accessed 31.10.12].
[2] Schmidt D. Low exergy systems for high-performance buildings and communities. Energy Build 2009;41:331–6.
[3] Szargut J. International progress in second law analysis. Energy 1980;5:709–18.
[4] Szargut J, Morris DR, Steward FR. Exergy analysis of thermal, chemical and metallurgical processes. New York: Hemisphere; 1988.
[5] Moran MJ. Availability Analysis:aguide to efficient energy use. revised ed. New York: ASME; 1990.
[6] Kotas YJ. The exergy method for thermal plant analysis. reprint ed. Malabar, FL: Krieger; 1995.
[7] Edgerton RH. Available energy and environmental economics. Toronto: D.C. Heath; 1992.
[8] Rosen MA, Dinçer I, Kanoglu M. Role of exergy in increasing efficiency and sustainability and reducing environmental impact. Energy Policy 2008;36:128–37.
[9] Hepbasli A. A review on energetic, exergetic and exergoeconomic aspects of geothermal district heating system (GDHSs). Energy Convers Manage 2010;51:2041–61.
[10] Hepbasli A, Akdemir O. Energy and exergy analysis of a ground source (geothermal) heat pump system. Energy Convers Manage 2004;45:737–53.
[11] Esen H, Inalli M, Esen M, Pihtili K. Energy and exergy analysis of a ground-coupled heat pump system with two horizontal ground heat exchangers. Build Environ 2007;42(10):3606–15.
[12] Fryda L. Integrated CHP with auto thermal biomass gasification and SOFC-MGT. Energy Convers Manage 2008;49:281–90.
[13] Abusoglu A, Kanoglu M. First and second law analysis of diesel engine powered cogeneration systems. Energy Convers Manage 2008;49:2026–31.
[14] Gonçalves P, Angrisani G, Rosselli C, Gaspar AR, Da Silva MG. Comparative energy and exergy performance assessments of a microcogenerator unit in different electricity mix scenarios. Energy Convers Manage 2013;73:195–206.
[15] Açikkalp E, Aras H, Hepblaski A. Advanced exergy analysis of an electricity-generating facility using by natural gas. Energy Convers Manage 2014;82:146–53.
[16] Koroneos C, Spachos T, Moussiopoulos N. Exergy analysis of renewable energy sources. Renewable Energy 2003;28:295–310.
[17] Kaviri AG, Jaafar MNM, Lazim TM, Barzegaravval H. Exergoenvironmental optimization of heat recovery steam generators in combined cycle power plant through energy and exergy analysis. Energy Convers Manage 2013;67:27–33.
[18] Kranzl L, Müller A, Kalt G. The trade-off between exergy-output and capital costs: the example of bioenergy utilization paths. In: 11th Symposium Energy Innovation, Graz, Austria, 2010 February 10–12.
[19] Tolga Balta A, Dincer I, Hepbasli A. Performance and sustainability assessment of energy options for building HVAC applications. Energy Build 2010;42:1320–8.
[20] Angelotti A, Caputo P. Energy and exergy analysis of heating and cooling systems in the italian context. In: Proceedings of Climamed, Genova, Italy, 2007, 5–7 September, p. 843–54.
[21] Björk F, Kilkiş Ş, Molinari M. Energy quality management and low energy architecture. In: ASES National Solar Conference, North Carolina, USA; 2011.
[22] Kilkiş Ş. A rational exergy management model for curbing building CO_2 emission. ASHRAE 2007;113:113–23.
[23] Molinari M. Exergy and parametric analysis: methods and concepts for a sustainable built environment. Stockolm, Sweden: Royale Institute of Technology; 2012.
[24] Molinari M. Exergy Analysis in Buildings: a complementary approach to energy analysis, Stockolm. Sweden: KTH- Stockolm; 2009.
[25] Kari A, Arto S. Distributed energy generation and sustainable development. Renew Sustain Energy Rev 2006;10:539–58.
[26] Akorede MF, Hizam H, Poresmaeil E. Distributed energy resources and benefits to the environment. Renew Sustain Energy Rev 2010;14:724–34.
[27] Pepermans G, Driesen J, Haesoldoncklx D, Belmans R, D'haeseleer W. Distributed generation: definition, benefits and issues. Energy Policy 2005;33:787–98.
[28] Esen H, Inalli M, Esen M. Technoeconomic appraisal of a ground source heat pump system for a heating season in eastern Turkey. Energy Convers Manage 2006;47(9–10):1281–97.
[29] Esen H, Inalli M, Esen M. A techno-economic comparison of ground-coupled and air-coupled heat pump system for space cooling. Build Environ 2007;42(5):1955–65.
[30] Esen M, Yuksel T. Experimental evaluation of using various renewable energy sources for heating a greenhouse. Energy Build. 2013;65:340–51.
[31] Söderman J, Pettersson F. Structural and operational optimisation of distributed energy systems. Appl Therm Eng 2006;26:1400–8.
[32] Yan B, Luh PB, Sun B, Song C, Dong C, Gan Z, et al. Energy-efficient management of eco-communities. In: Proceedings of IEEE CASE; Madison, USA, 2013 August 17–20.
[33] Guan X, Xu Z, Jia Q. Energy-efficient buildings facilitated by microgrid. IEEE Trans Smart Grid 2011;1:466–73.
[34] Yan B, Luh PB, Bragin MA, Song C, Dong C, Gan Z. Energy-efficient building clusters. In: Proceedings of IEEE CASE Taiwan; Taipei, Taiwan, 2014 August 18–22.
[35] Hongbo R, Weisheng Z, Ken'ichi N, Weijun G, Qiong W. Multi-objective optimization for the operation of distributed energy systems considering economic and environmental problems. Appl Energy 2010;87:3642–51.
[36] Ramirez-Elizondo LM, Paap GC, Ammerlaan R, Negenborn RR, Toonssen R. On the energy, exergy and cost optimization of multi-energy-carrier power systems. Int J Exergy 2013;13:364–85.
[37] Krause T, Kienzle F, Art S, Andersson G. Maximizing exergy efficiency in multi-carrier energy systems. In: Proceedings of IEEE Power and Energy Society General Meeting; Minneapolis, USA, 2010 June 25–29.
[38] Di Somma M, Yan B, Luh PB, Bragin MA, Bianco N, Graditi G, Mongibello L, Naso V. Exergy-efficient Management of Energy Districts. In: Proceedings of the 11th World Congress on Intelligent Control and Automation, Shenyang, China, 2014, 29 June – 4 July, p. 2675–80.
[39] Hawkes AD, Leach MA. Modelling high level system design and unit commitment for a microgrid. Appl Energy 2009;86:1253–65.
[40] Mehleri ED, Sarimveis H, Markatos NC, Papageorgiou LG. A mathematical programming approach for optimal design of distributed energy systems at the neighbourhood level. Energy 2012;44:96–104.
[41] Weber C, Shah N. Optimisation based design of a district energy system for an eco-town in the United Kingdom. Energy 2011;36:1292–308.
[42] Zhou Z, Liu P, Li Z, Ni W. An engineering approach to the optimal design of distributed energy systems in China. Appl Therm Eng 2013;53:387–96.
[43] Kong XQ, Wang RZ, Huang XH. Energy optimization for a CCHP system with available gas turbines. Appl Therm Eng 2005;25:377–91.
[44] Aiying R, Risto L. An effective heuristic for combined heat-and-power production planning with power ramp constraints. Appl Energy 2007;84:307–25.
[45] Kriett P, Salani M. Optimal control of a residential microgrid. Energy 2012;42(1):321–30.
[46] Brahman F, Jadid, S. Optimal energy management of hybrid CCHP and PV in a residential building. In: Proceedings of 19th IEEE Conference on Electrical Power Distribution Networks, 2014 May 6–7. p. 19–24.
[47] Lu H, Alanne K, Martinac I. Energy quality management for building clusters and districts (BCDs) though multi-objective optimization. Energy Convers Manage 2014;79:525–33.
[48] Angelotti A, Caputo P. The exergy approach for the evaluation of heating and cooling technologies, first results comparing steady state and dynamic simulations. In: Proceedings of the 2nd PALENC and 28th AIVC Conference, vol I; 2007 September 27–29; Crete Island, Greece; p. 59–64.
[49] Torìo H, Angelotti A, Schmidt D. Exergy analysis of renewable energy-based climatisation systems for buildings: a critical view. Energy Build 2009;41:248–71.
[50] Torìo H, Schmidt D. Framework for analysis of solar energy systems in the built environment from an exergy perspective. Renewable Energy 2010;35:2689–97.
[51] ASHRAE International Weather files for Energy Calculations (IWEC weather files). Users manual and CD-ROM, American Society of Heating, Refrigerating and Air-Conditioning Engineers, Atlanta, GA, USA, 2001.
[52] ANSI/ASHRAE Standard 55. Thermal Environmental Conditions for Human Occupancy; 2013. <http://www.techstreet.com/products/1868610>.
[53] Beijing Municipal Commission of Development & Reform, Current prices for Public commodities. <http://www.bjpc.gov.cn/english/>.
[54] Kaushik SC, Reddy VS, Tyagi SK. Energy and exergy analyses of thermal power plants: a review. Renew Sustain Energy Rev 2011;15:1857–72.
[55] Forum – Oxford Institute for Energy Studies, Issue 95, February 2014. <http://www.oxfordenergy.org/wpcms/wp-content/uploads/2014/04/OEF-95.pdf>.
[56] Chau J, Sowlati T, Sokhansanj S, Preto F, Melin S, Bi S. Techno-economic analysis of wood biomass boilers for the greenhouse industry. Appl Energy 2009;86:364–71.
[57] Emerson DB, Whitworth BA. Summary of micro-turbine technology. Orlando, Florida: Summit; 1998.
[58] Broad Air Conditioning Company. <www.broad.com/english/product1.htm>.
[59] Kinab E, Marchio D, Rivière P, Zoughaib A. Reversible heat pump model for seasonal performance optimization. Energy Build 2010;42:2269–80.
[60] Catalog of CHP technologies, U.S. Environmental Protection Agency Combined Heat and Power Partnership. <http://www.epa.gov/chp/documents/catalog_chptech_5.pdf>.